THE JOURNAL OF BIOLOGICAL CHEMISTRY VOL. 285, NO. 32, pp. 24466–24476, August 6, 2010

Identification and Characterization of a Novel Human PP1 Phosphatase Complex*

Received for publication, February 2, 2010, and in revised form, May 7, 2010 Published, JBC Papers in Press, June 1, 2010, DOI 10.1074/jbc.M110.109801

Jeong-Heon Lee[‡1], **Jinsam You**[§], **Erika Dobrota**[‡], **and David G. Skalnik**[‡]

From the [‡]*Wells Center for Pediatric Research, Section of Pediatric Hematology/Oncology, Departments of Pediatrics and Biochemistry and Molecular Biology, Indiana University School of Medicine, Indianapolis, Indiana 46202 and* [§]*Monarch LifeSciences, Indianapolis, Indiana 46202*

Mammalian Wdr82 is a regulatory component of the Setd1a and Setd1b histone H3-lysine 4 methyltransferase complexes and is implicated in the tethering of Setd1 complexes to transcriptional start sites of active genes. In the studies reported here, immunoprecipitation and mass spectrometry analyses reveal that Wdr82 additionally associates with multiple protein complexes, including an RNA polymerase II complex, four distinct histone H3-Lys[4] methyltransferase complexes, protein phosphatase 1 (PP1)-associated proteins, a chaperonin-containing Tcp1 complex, and other uncharacterized proteins. Further characterization of the PP1-associated proteins identified a stable multimeric complex composed of regulatory subunits PNUTS, Tox4, and Wdr82 and a PP1 catalytic subunit (denoted as the PTW/PP1 phosphatase complex). The PTW/PP1 complex exhibits *in vitro* phosphatase activity in a PP1-dependent manner. Analysis of protein-protein interactions reveals that PNUTS mediates phosphatase complex formation by providing a binding platform to each component. The PNUTS and Tox4 subunits are predominantly associated with the PTW/PP1 phosphatase complex in HEK293 cells, and the integrity of this complex remains intact throughout cell cycle progression. Inducible expression of a PP1 interaction-defective form of PNUTS (W401A) or small interfering RNA-mediated depletion of PNUTS in HEK293 cells causes cell cycle arrest at mitotic exit and apoptotic cell death. PNUTS (W401A) shows normal association with chromosomes but causes defects in the process of chromosome decondensation at late telophase. These data reveal that mammalian Wdr82 functions in a variety of cellular processes and reveal a potential role of the PTW/PP1 phosphatase complex in the regulation of chromatin structure during the transition from mitosis into interphase.

Protein phosphatase 1 (PP1)[2] is a serine/threonine protein phosphatase involved in diverse cellular processes, such as transcription, replication, pre-mRNA splicing, protein synthesis, muscle contraction, carbohydrate metabolism, neuronal signaling, cell survival, and cell cycle progression (1–3). Mammals express three PP1 catalytic isoforms, PP1α, PP1γ, and PP1β/σ, which show distinct subcellular localization patterns (4, 5). PP1 catalytic isoforms do not exist freely in cells but rather associate with regulatory subunits to form distinct multimeric holoenzymes. In general, PP1 regulatory subunits function as signaling modules by regulating the enzymatic activity or targeting of catalytic subunits to specific substrates (6, 7). PP1 is involved in cell cycle progression, especially during mitosis and mitotic exit, and dysregulation of PP1 activity causes mitotic arrest or deficient cytokinesis in mammals (3, 8, 9). PP1 is associated with multiple mitotic structures, such as chromosomes, centrosomes, and spindles (4, 8, 10), and is implicated as a major phosphatase acting on phosphoproteins at mitotic exit (11–14). However, the specific regulatory or targeting subunits required for this activity are not well understood. Therefore, the characterization of multimeric PP1 complexes is essential for understanding PP1 functions in specific biological pathways.

Numerous chromatin-associated PP1 regulatory subunits have been identified and often contain histone-modifying or chromatin-remodeling activities (15). PP1 nuclear targeting subunit (PNUTS), also known as PPP1R10, p99, FB19, or CAT 53, was originally identified as a mammalian nuclear PP1-binding protein (16–18). PNUTS contains several functional domains, including an N-terminal transcription elongation factor S-II (TFS2N) domain implicated in the transcriptional initiation or elongation of RNA polymerase (pol) II (19), a putative zinc finger domain, a consensus PP1-binding RV*X*F motif, and C-terminal RGG motifs that interact with homopolymeric RNA (17, 20). PNUTS is ubiquitously expressed and tightly associates with chromatin during interphase but is excluded from chromosomes at early mitosis and is reloaded onto chromosomes during the transition from mitosis to interphase (21). PNUTS also enhances *in vitro* chromosome decondensation in a PP1-dependent manner. These observations led to the hypothesis that PNUTS may be a regulator of signaling events promoting chromosome decondensation as cells reenter interphase (21). PNUTS is also implicated in regulation of cell cycle progression and apoptosis. Interaction of PNUTS with PP1 inhibits dephosphorylation of the retinoblastoma cell cycle

* This work was supported in part by the Riley Children's Foundation, the Lilly Endowment, National Science Foundation Grant MCB-0641851 (to D. G. S.), and a Showalter Trust award (to J.-H. L.).

[1] To whom correspondence should be addressed: Wells Center for Pediatric Research, Dept. of Pediatrics, Indiana University School of Medicine, Indianapolis, IN 46202. Fax: 317-274-8928; E-mail: jeonglee@iupui.edu.

[2] The abbreviations used are: PP1, protein phosphatase 1; PNUTS, protein phosphatase-1 nuclear targeting subunit; HEK, human embryonic kidney; pol, polymerase; PBS, phosphate-buffered saline; GST, glutathione *S*-transferase; PIPES, 1,4-piperazinediethanesulfonic acid; PI, propidium iodide; DAPI, 4′,6-diamidino-2-phenylindole; CTD, C-terminal domain of RNA pol II; GFP, green fluorescent protein; MAPK, mitogen-activated protein kinase; siRNA, small interfering RNA; aa, amino acids; PTW/PP1, multimeric complex composed of regulatory subunits PNUTS, Tox4, and Wdr82 and a PP1 catalytic subunit.

regulatory protein (22–24), and siRNA-mediated depletion of PNUTS causes apoptosis in an retinoblastoma-dependent manner in cancer cells (24). Also, the gene encoding PNUTS is induced by hypoxia, and PNUTS regulates the phosphorylation and apoptotic activities of p53 under hypoxic conditions (25).

WD40 domains are found in a large family of proteins with diverse biologic functions, including adaptor/regulatory modules in signal transduction, pre-mRNA processing, cytoskeleton assembly, and cell cycle control (26, 27). WD40 domain-containing proteins typically contain seven WD40 repeats that form β-propeller-like platforms to which other proteins bind. The WD40 repeat propeller structure is a versatile module for recognition of post-translational protein modifications, such as H3-Lys^4 methylation or phosphorylated serine/threonine residues (28–31). The WD40 repeat protein Wdr82 is a component of the Setd1a and Setd1b histone H3-Lys^4 methyltransferase complexes and specifically recognizes the Ser^5-phosphorylated C-terminal domain (CTD) of RNA pol II and directs the Setd1 complexes to transcriptional start sites of active genes (32–34). Swd2, a yeast homologue of Wdr82, is implicated in histone H3-Lys^4 trimethylation at the 5′-region of active genes and transcriptional termination at the 3′-end of genes. Swd2 is a component of two distinct complexes, the Set1/COMPASS H3-Lys^4 methyltransferase and the APT (associated with Pta1) subcomplex of the cleavage and polyadenylation factor (35–39). Recently, Swd2 was implicated in histone H2B ubiquitination-dependent histone H3-Lys^4 methylation at the 5′-region of active genes, a process known as histone cross-talk (40, 41).

In this study, mammalian Wdr82-associated proteins were identified using affinity purification and mass spectrometry to gain further insights into Wdr82 function. In addition to the previously reported interaction with Setd1 histone H3-Lys^4 methyltransferase complexes, these studies reveal that Wdr82 associates with PP1 catalytic and regulatory subunits. Further characterization revealed a stable multimeric PP1 complex composed of PNUTS, Tox4 (also known as Lcp1 (Langerhans cell protein 1)), and Wdr82. PNUTS mediates complex formation by providing a binding platform for each component. Inducible expression of a PP1 interaction-defective form of PNUTS (W401A) causes cell cycle arrest at mitosis and cell death. PNUTS (W401A) exhibits normal association with chromosomes but causes defects in the process of chromosome decondensation at late telophase, indicating that this PP1 phosphatase complex plays a role in the control of chromatin structure and cell cycle progression during the transition from mitosis into interphase.

EXPERIMENTAL PROCEDURES

Cell Lines—Human embryonic kidney cells (HEK293) were cultured and maintained as described (42). T-REx HEK293 cells that constitutively express the tetracycline repressor (Invitrogen) were maintained in Dulbecco's modified Eagle's medium supplemented with 10% bovine calf serum and 5 μg/ml blasticidin (Invitrogen). To establish inducible cells, T-REx HEK293 cells were transfected as described (33) and selected in medium containing 200 μg/ml hygromycin B (Sigma) and 5 μg/ml blasticidin. Inducible T-REx cell lines were maintained in Dulbecco's modified Eagle's medium containing 50 μg/ml hygromycin B and 5 μg/ml blasticidin.

T-REx HEK293 cells were synchronized by successive thymidine and nocodazole blocks as described (43). Briefly, cells were cultured in complete medium containing 2 mM thymidine (Sigma) for 16 h. Cells were washed and incubated in fresh medium for 2 h and were incubated in medium containing 100 ng/ml nocodazole (Sigma) for 12 h. After washing with phosphate-buffered saline (PBS) and fresh medium, cells were released from mitotic arrest by incubating with fresh medium.

Plasmid Construction—The cDNA of human Wdr82 (32) was subcloned into pcDNA5/TO vector (Invitrogen) containing an N-terminal FLAG epitope. Human Tox4, mouse PNUTS, and human Scp1 (small C-terminal domain phosphatase-1), human NIPP1 (nuclear inhibitor of protein phosphatase-1), human PP1α, human PP1β, and human PP1γ cDNAs were amplified from expressed sequence-tagged clones obtained from the American Type Culture Collection. The cDNAs were subcloned into the pcDNA3 vector, which contains an N-terminal FLAG epitope, and were subsequently subcloned into the pcDNA5/TO vector (Invitrogen). Site-directed mutagenesis was performed on the RV*X*F motif of PNUTS using primers that mutate a tryptophan residue to alanine using the QuikChange site-directed mutagenesis kit (Stratagene) in accordance with the protocol provided by the manufacturer. PNUTS (W401A) cDNA was subcloned into the pcDNA5/TO vector, which contained an N-terminal FLAG epitope tag or green fluorescent protein (GFP). Various deletion constructs of PNUTS cDNA were subcloned into the pcDNA3 vector (Invitrogen) with an N-terminal FLAG epitope using PCR and restriction enzyme digestions. The nucleotide sequence of all constructs was confirmed.

Identification of Protein Complexes by Mass Spectrometry—T-REx HEK293 cells that inducibly express FLAG-Wdr82, FLAG-PNUTS, FLAG-Tox4, or empty vector were treated with 1 μg/ml doxycyline for 3 days. Nuclear extracts were prepared as described previously (32) in extraction buffer (10 mM PIPES, pH 7.0, 300 mM NaCl, 300 mM sucrose, 3 mM $MgCl_2$, 1 mM EGTA), supplemented with the protease inhibitors leupeptin, aprotinin, pepstatin (1 μg/ml each), 1 mM phenylmethylsulfonyl fluoride, and 0.5% Triton X-100), and anti-FLAG M2 agarose beads (Sigma) were added, incubated for 3 h, and extensively washed. Bound proteins were eluted with extraction buffer containing 250 μg/ml FLAG peptide (Sigma). Proteins were denatured and separated by 4–12% SDS-PAGE and stained with Coomassie Brilliant Blue. Protein bands were excised and processed for in-gel trypsin digestion. Peptides were extracted with 0.1% formic acid for 30 min at 37 °C and injected into a 75 μm × 5-cm C-18 reverse-phase column (Waters, Picofrit column) and were eluted with a gradient of 5–45% acetonitrile developed over 30 min at a flow rate of 250 nl/min using an Agilent 1100 series nanopump. The column was interfaced with an LTQ ion trap mass spectrometer (Thermo), and data were collected in the triple play mode. Tandem mass spectra were searched against the IPI human protein data base (version 3.57) with SEQUEST (version 2.7) and X!Tandem.

Immunoprecipitation and Western Blotting Analysis—Nuclear or whole cell extracts were prepared as described (32). Cell extracts were incubated with anti-FLAG M2-agarose beads for 3 h and extensively washed. Bound proteins were eluted with SDS sample buffer. For PNUTS, Tox4, Setd1a, and Setd1b immunoprecipitations, nuclear extracts were precleared and incubated with antibodies for 3 h and incubated with protein A-agarose beads (Roche Applied Science) for 1 h. Protein A-agarose beads were washed four times with the extraction buffer containing 300 mM NaCl. Proteins were eluted with SDS sample buffer and analyzed by Western blotting. Antisera utilized are as follows. Anti-FLAG (mouse monoclonal M2) antibody was obtained from Sigma. Antisera directed against Ash2L, Rbbp5, Mll1, Mll2, PP1α, PP1β, PP1γ, and Tcp1α were obtained from Bethyl Laboratories. Anti-Tox4 and anti-Rbp2 antisera were obtained from Aviva Systems Biology, LLC (San Diego, CA). Anti-Rbp1 antiserum was obtained from Santa Cruz Biotechnology, Inc. (Santa Cruz, CA). Anti-Ser^5-phosphorylated RNA pol II CTD (monoclonal H14) was obtained from Covance Ltd. (Berkeley, CA). Anti-acetylated histone H3 antibody was obtained from Upstate Biotechnology, Inc. (Lake Placid, NY). Anti-NuMA (Ab-1) was obtained from EMD Biosciences, Inc. (La Jolla, CA). Anti-PNUTS antiserum was kindly provided by Dr. Mathieu Bollen (Catholic University of Leuven, Belgium). Anti-Mll4 and anti-Ptip antisera were kindly provided by Dr. Kai Ge (National Institutes of Health). Generation of antisera directed against Setd1a, Setd1b, Cfp1, Wdr5, and Wdr82 was previously described (32, 33).

Purification of Recombinant Proteins and in Vitro Pull-down Assay—The cDNA encoding PP1α was subcloned into the pGEX 4T vector (Amersham Biosciences), and constructs were transformed into *Escherichia coli* BL21 cells. Transformants were grown and induced with 0.2 mM isopropyl-β-D-thiogalactoside for 4 h at 25 °C. Glutathione *S*-transferase (GST)-PP1α fusion protein was purified using glutathione-agarose affinity bead (Sigma), and purified protein was dialyzed against PBS containing 10% glycerol. cDNAs encoding PNUTS, Tox4, or NIPP1 were subcloned into the pFASTBAC HTa vector (Invitrogen). Generation of recombinant baculovirus and expression of recombinant proteins in *Sf9* cells were performed according to the manufacturer's instructions. For the purification of recombinant proteins, *Sf9* cells were harvested and resuspended in 10 ml of lysis buffer (50 mM sodium phosphate, pH 8.0, 300 mM NaCl, 10 mM imidazole, 1 mM phenylmethylsulfonyl fluoride, and 0.05% Tween 20). Cells were homogenized using a Dounce homogenizer, and lysates were centrifuged. Supernatants were incubated with Ni^{2+}-nitrilotriacetic acid-agarose beads (Qiagen, Valencia, CA) for 4 h at 4 °C, and beads were extensively washed using wash buffer (50 mM sodium phosphate, pH 8.0, 300 mM NaCl, 20 mM imidazole, and 0.05% Tween 20). Bound proteins were eluted with elution buffer (50 mM sodium phosphate, pH 8.0, 300 mM NaCl, 250 mM imidazole, and 0.05% Tween 20) and dialyzed against PBS containing 10% glycerol. Purification of recombinant FLAG-Wdr82 from insect cells was performed as described previously (34).

For FLAG pull-down assays, purified proteins were incubated in 1 ml of pull-down buffer (20 mM Tris-HCl, pH 8.0, 150 mM NaCl, 2 mM EDTA, 0.2% Nonidet P-40, and 0.5% deoxycholate) for 2 h, and anti-FLAG M2-agarose beads were added and incubated at 4 °C for 2 h. Beads were extensively washed with pull-down buffer, and bound proteins were denatured by SDS sample buffer. Proteins were separated by SDS-PAGE and stained with Coomassie Brilliant Blue. For GST pull-down assays, glutathione-agarose beads were used, and reactions were performed as described above.

Protein Phosphatase Assay—In vitro phosphatase activity of the PP1 complex was analyzed using Ser^5-phosphorylated recombinant GST-CTD as a substrate. pGST-mCTD, a bacterial expression vector expressing full-length mouse CTD, was kindly provided by Dr. Michael Dahmus (University of California, Davis, CA). Purified GST-CTD was phosphorylated by MAPK (New England Biolabs, Beverly, MA) as described previously (34). Recombinant inhibitor 2, a highly specific and strong PP1 inhibitor (44), was purchased from New England Biolabs. NIPP1, another specific PP1 inhibitor (45), was purified from insect *Sf9* cells infected by recombinant baculovirus encoding His-tagged NIPP1.

Nuclear extracts isolated from inducible T-REx HEK293 stable cell lines were subjected to FLAG immunoprecipitation. Bound proteins were eluted by FLAG peptide after extensive washing, and FLAG immunoprecipitates were used for an *in vitro* phosphatase assay. MAPK-treated GST-CTD was incubated with FLAG immunoprecipitates in the absence or presence of inhibitor 2 or NIPP1 at 30 °C for 1 h in PP1 reaction buffer (50 mM HEPES, pH 7.5, 0.1 mM EDTA, 5 mM dithiothreitol, 0.025% Tween 20, and 1 mM $MnCl_2$). The reaction products were analyzed by Western blotting using antiserum directed against Ser^5-phosphorylated CTD (monoclonal H14, Covance Ltd.).

siRNA-mediated depletion of PNUTS—HEK293 cells were transfected by control (D-001206–14) or PNUTS (M-011358) SMART pool siRNAs (Dharmacon) according to the manufacturer's instructions using DharmaFECT transfection reagent (Dharmacon) and analyzed after 3 days.

Flow Cytometric Analysis—For cell cycle analysis, cells were harvested, washed twice with PBS, fixed with cold 70% ethanol, and incubated in PBS containing 0.3% Nonidet P-40, 0.5 mg/ml RNase A, and 50 μg/ml propidium iodide (PI) for 30 min on ice. Following staining, samples were analyzed for cell cycle distribution using a FACScan flow cytometer (BD Biosciences) and ModFit LT software (Verity Software, Topsham, ME). Apoptotic cells were detected using an Annexin V-FLUOS and PI staining kit (Roche Applied Science) according to the manufacturer's instructions. Apoptotic cells were defined as Annexin V-positive and PI-negative cells. Statistical significance was assessed by one-tailed *t* tests, with a *p* value of <0.05 interpreted as statistical significance.

Immunofluorescence and Confocal Microscopy—T-REx HEK293 cells were cultured on glass bottom collagen-coated dishes and were analyzed as described (42) with slight modifications. Briefly, cells were fixed with 4% (v/v) paraformaldehyde in PBS, permeabilized with 0.2% Triton X-100 in PBS, and then incubated with blocking solution (PBS containing 2.5% normal bovine serum and 0.2% Tween 20) for 1 h. Anti-FLAG mouse IgG (1:1000, 3.5 μg/ml) (Sigma) was added and incubated for 2 h at room temperature. Cells were then

washed three times with PBS containing 0.2% Tween 20. Bovine anti-mouse IgG-fluorescein isothiocyanate (2 μg/ml in blocking solution) was added and incubated for 1 h. Cells were washed three times, and nuclei were stained with 0.1 μg/ml 4,6-diamidino-2-phenylindole (DAPI) in PBS for 5 min, followed by washing with PBS. Cells were scanned with a Zeiss LSM 510 laser-scanning confocal microscope (Indiana Center for Biological Microscopy). For detection of the GFP-PNUTS (W401A) mutant, cells were fixed, permeabilized, and scanned with a confocal microscope after staining with DAPI as described above.

RESULTS

Affinity Purification and Identification of Wdr82-associated Proteins—We and others previously reported that mammalian Wdr82 protein specifically associates with the Setd1 histone H3-Lys^4 methyltransferase complexes (32, 33, 46). Wdr82 recognizes the Ser^5-phosphorylated form of RNA pol II CTD, which is associated with an early step of transcription elongation and targets the Setd1a and Setd1b methyltransferase complexes to transcription start sites of active genes (34). Wdr82-associated proteins were purified and identified to further investigate the cellular function(s) of Wdr82. Nuclear extracts isolated from T-REx HEK293 cell lines expressing FLAG-Wdr82 or carrying the empty vector were subjected to FLAG immunoprecipitation (Fig. 1*A*). In addition to FLAG-tagged Wdr82, 16 protein bands were detected that were not present in the control immunopurification. Mass spectrometry analysis of protein bands identified a total of 29 unique proteins, with detection of multiple peptides for each protein (Fig. 1*A*). These were grouped into five categories based on known biological activities: the chaperonin-containing Tcp1 complex (47), four distinct histone H3-Lys^4 methyltransferase complexes (Setd1a, Setd1b, Mll3 (mixed lineage leukemia), and Mll4) (32, 33, 48, 49), PP1-regulatory proteins (PNUTS and Tox4 (also known as Lcp1 and KIAA0737)) and PP1 catalytic subunits (50), RNA pol II catalytic core subunits (Rbp1 and Rbp2) (34), and currently uncharacterized proteins (Rbm10 and C19orf7) (Fig. 1*B*).

Representative components of each putative Wdr82 complex were analyzed by Western blotting following immunoprecipitation to assess the authenticity of protein interactions identified by mass spectrometry analysis (Fig. 1*C*). In all cases, proteins identified by mass spectrometry were detected in the FLAG-Wdr82 immunoprecipitates but were not detected in FLAG immunoprecipitates prepared from cells carrying the empty expression vector. For example, FLAG immunoprecipitation recovers Tcp1α, a component of the chaperonin-containing Tcp1 complex (47). For the histone methyltransferase complexes, immunoprecipitation recovered C*XX*C finger protein 1 (Cfp1), a unique component of the Setd1a/b complexes; the Setd1a and Setd1b proteins (32, 33); Pax transactivation domain-interacting protein (Ptip), a unique component of the Mll3 and Mll4 complexes (48, 49); the Mll4 protein; and Ash2L, Rbbp5, and Wdr5 components of Set1-like methyltransferase complexes (51). However, Mll1 and Mll2, other members of the Set1-like histone H3-Lys^4 methyltransferase family that were not detected in the mass spectrometry analysis (Fig. 1*A*), were

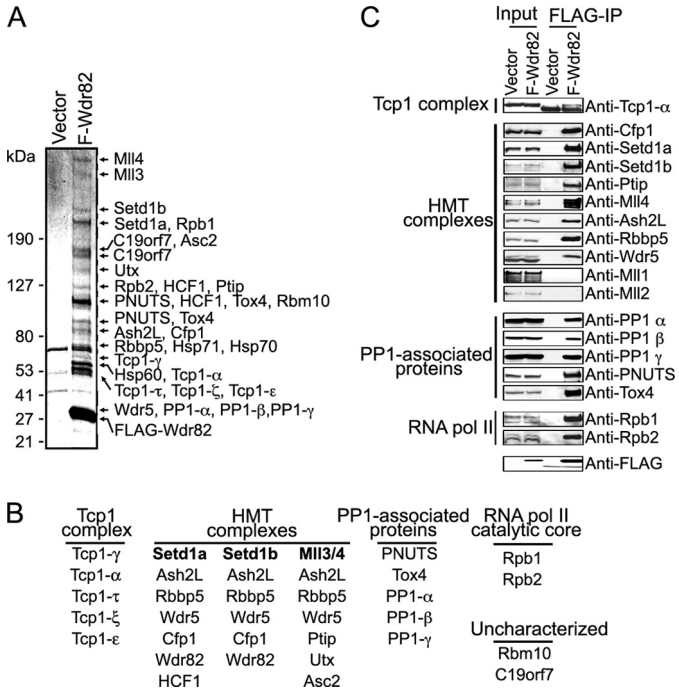

FIGURE 1. **Wdr82 is associated with multiple protein complexes.** *A*, T-REx HEK293 stable cell lines that express FLAG-Wdr82 or empty vector were induced with 1 μg/ml doxycycline for 3 days. Nuclear extracts were prepared and subjected to FLAG immunoprecipitation (*FLAG-IP*), and bound proteins were eluted by FLAG peptide after extensive washing. Proteins were analyzed by SDS-PAGE and stained with Coomassie Brilliant Blue. Protein bands were excised and processed for in-gel trypsin digestion. Peptides were analyzed by quadrupole time-of-flight mass spectrometry, and proteins were identified. *B*, identified proteins are classified into five categories based on known biological activities. *C*, T-REx HEK293 stable cell lines that express FLAG-Wdr82 or empty vector were induced with 1 μg/ml doxycycline for 3 days. Nuclear extracts were subjected to FLAG immunoprecipitation, and immunoprecipitates were analyzed by Western blotting for representative proteins of each complex class.

also not found in the FLAG-Wdr82 immunoprecipitate (Fig. 1*C*), demonstrating that Wdr82 specifically associates with the Setd1a, Setd1b, Mll3, and Mll4 methyltransferase complexes. For the PP1 complex, three different isoforms of PP1 and PP1-regulatory proteins, such as PNUTS and Tox4, were detected by specific antisera in the FLAG-Wdr82 immunoprecipitate. Finally, large and small subunits of RNA pol II were detected in the FLAG-Wdr82 immunoprecipitate, as reported previously (34).

Characterization of a Putative Phosphatase Complex Containing PNUTS, Tox4, Wdr82, and PP1—Co-immunoprecipitation studies were performed to further assess the Wdr82-containing PP1 complex. Nuclear extracts derived from HEK293 cells were subjected to immunoprecipitation using antisera directed against endogenous Tox4, PNUTS, Setd1a, or Setd1b, and immunoprecipitates were analyzed by Western blotting. Fig. 2*A* demonstrates that endogenous Wdr82 associates with Tox4, PNUTS, Setd1a, and Setd1b. Rbbp5, a common component of Set1-like histone H3-Lys^4 methyltransferase complexes, associates with Setd1a and Setd1b as previously reported (32, 33) but does not associate with Tox4 or PNUTS. Also, Tox4 and PNUTS associate with PP1 but do not associate with Setd1a and Setd1b. Taken together, these results indicate that the PP1 and Setd1 complexes both contain Wdr82 but are physically distinct. Last, Tox4 associates with PNUTS, PP1, and Wdr82.

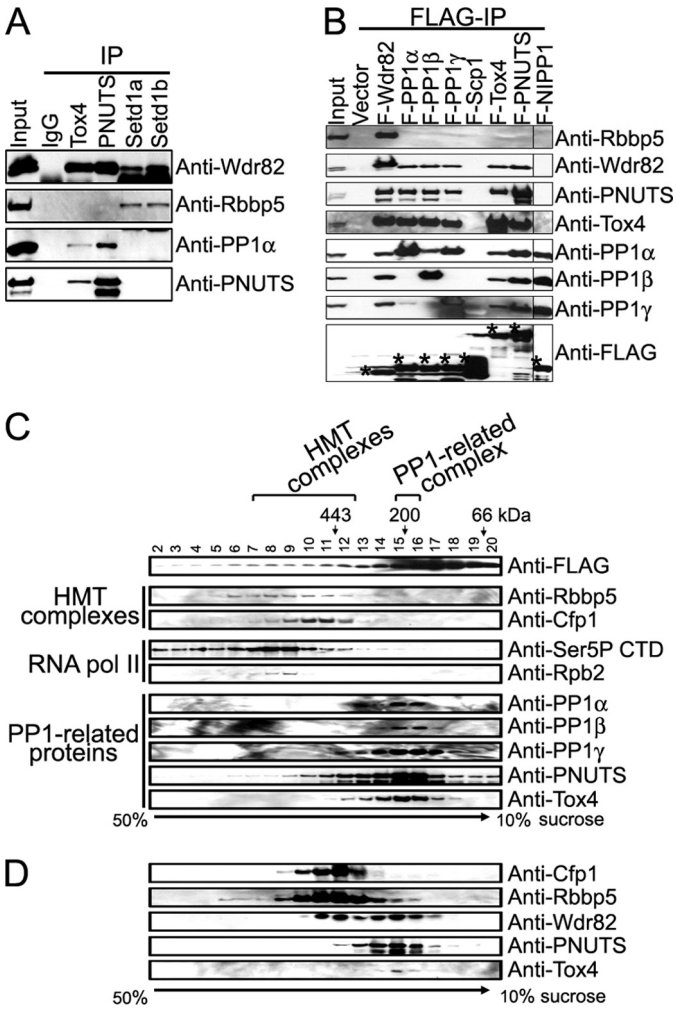

FIGURE 2. **Wdr82 forms a complex with PP1 catalytic and regulatory subunits.** *A*, endogenous PNUTS and Tox4 associate with PP1 and Wdr82. Nuclear extracts isolated from HEK293 cells were subjected to immunoprecipitation (*IP*) using antisera directed against Tox4, PNUTS, Setd1a, or Setd1b. Immunoprecipitates were analyzed by Western blotting using the indicated antisera. *B*, PNUTS, Tox4, Wdr82, and PP1 catalytic subunits exhibit reciprocal immunoprecipitation. Inducible T-REx HEK293 stable cell lines that express empty vector or the indicated FLAG-tagged protein were induced by 1 μg/ml doxycycline for 3 days. Nuclear extracts were subjected to FLAG immunoprecipitation, and immunoprecipitates were analyzed by Western blotting using the indicated antisera. *Asterisks* in the FLAG Western blot indicate the expected size of each FLAG-tagged protein. *C*, PNUTS, Tox4, Wdr82, and PP1 catalytic subunits co-migrate following sucrose gradient fractionation. T-REx HEK293 cells that express FLAG-Wdr82 were induced with 1 μg/ml doxycycline for 3 days. Nuclear extracts were prepared and subjected to FLAG immunoprecipitation, and bound proteins were eluted by FLAG peptide. Wdr82-associated proteins were loaded onto 10–50% sucrose gradients and analyzed by equilibrium centrifugation, as described previously (32). Equal volumes of each fraction were analyzed by Western blotting. Migration of RNA pol II subunits, histone methyltransferase complex components, and PP1-associated proteins such as PNUTS, Tox4, and PP1 catalytic subunits are shown in the gradient. Molecular markers were applied to a parallel gradient. *D*, endogenous PNUTS, Tox4, and Wdr82 co-migrate following sucrose gradient fractionation analysis. Nuclear extracts from HEK293 cells were loaded onto 10–50% sucrose gradients and analyzed by equilibrium centrifugation. Fractions were collected, and equal volumes of each fraction were analyzed by Western blotting using the indicated antisera.

Additional studies were performed to assess the interaction specificity of PP1-associated proteins. Inducible T-REx HEK293 cell lines were generated that express FLAG-tagged versions of Wdr82, PP1α, PP1β, PP1γ, Scp1 (an unrelated phosphatase) (52), Tox4, PNUTS, or the PP1 inhibitor NIPP1. Cells were induced with 1 μg/ml doxycycline for 3 days, nuclear extracts were isolated and subjected to FLAG immunoprecipitation, and immunoprecipitates were analyzed by Western blotting (Fig. 2*B*). Consistent with the results presented in Fig. 2*A*, Rbbp5 associates with Wdr82 but not with other PP1-associated proteins. The Scp1 phosphatase does not associate with any of the proteins tested. NIPP1, a known PP1 regulatory subunit, interacts with all three catalytic PP1 subunits, as reported previously (45), but does not associate with Wdr82, Tox4, or PNUTS. Importantly, Wdr82, Tox4, PNUTS, PP1α, PP1β, and PP1γ exhibit reciprocal immunoprecipitation, indicating that PNUTS, Tox4, Wdr82, and a PP1 catalytic subunit comprise a complex, hereafter denoted as the PTW/PP1 phosphatase complex.

To further characterize the PTW/PP1 phosphatase complex, purified FLAG-Wdr82-associated proteins recovered from T-REx HEK293 cells were analyzed by Western blotting following sucrose gradient fractionation, as described previously (32) (Fig. 2*C*). FLAG-Wdr82 was found in all fractions, with the majority in the 60–200 kDa size range. Rbbp5 and Cfp1, components of Setd1 histone H3-Lys^4 methyltransferase complexes, were detected in the ~450 kDa size range, and RNA pol II components, such as Rpb1 and Rpb2, were detected in a higher size range. In contrast, PP1α, PP1β, PP1γ, PNUTS, and Tox4 co-migrate in the ~200 kDa size range, providing further evidence that the Wdr82-Setd1 and Wdr82-PP1 complexes are physically distinct.

Similar studies were performed to assess the size of endogenous Wdr82-containing complexes (Fig. 2*D*). Nuclear extracts from HEK293 cells were fractionated by sucrose gradient equilibrium centrifugation as described above, and each fraction was analyzed by Western blotting. Consistent with the results presented in Fig. 2*C*, Cfp1 and Rbbp5, components of Setd1 histone H3-Lys^4 methyltransferase complexes, migrate in the 450 kDa size range. A small amount of Rbbp5 was also detected in a size range greater than 450 kDa. PNUTS and Tox4 are found in the 200 kDa size range, similar to what was found following FLAG-Wdr82 immunoprecipitation. Endogenous Wdr82 is found equally distributed between the 200 and 450 kDa size ranges, suggesting that Wdr82 is present in multiple complexes. These results indicate that PNUTS, Tox4, and Wdr82 form a stable PTW/PP1 phosphatase complex of ~200 kDa. Summation of the predicted size of the four complex components (~235 kDa) agrees well with the observed mass of the PTW/PP1 phosphatase complex and suggests a 1:1 stoichiometry for the subunits. It is noteworthy that the PTW/PP1 phosphatase complex identified here is a mixture of three distinct complexes containing either the PP1α, PP1β, or PP1γ catalytic subunit.

To further assess the interaction complexity of PTW/PP1 complex components, FLAG-PNUTS and FLAG-Tox4-associated proteins were isolated from T-REx HEK293 cell lines. Purified proteins were separated on SDS-PAGE and visualized by staining with Coomassie Brilliant Blue (Fig. 3*A*). Migration patterns of PNUTS- and Tox4-associated proteins on SDS-PAGE are similar to each other. Protein bands that are not present in the control immunopurification were further processed for protein identification by mass spectrometry. PNUTS associates

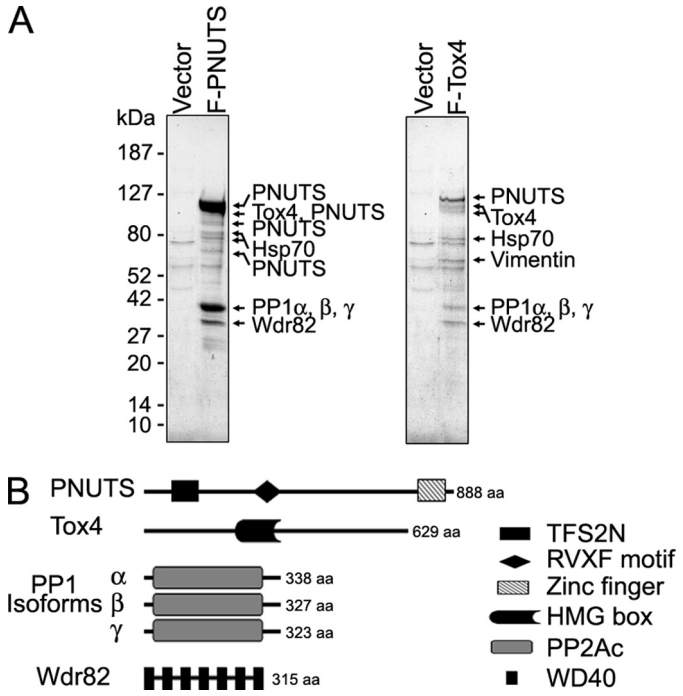

FIGURE 3. **PNUTS and Tox4 interact nearly exclusively with components of the PTW/PP1 phosphatase complex.** *A*, identification of PNUTS- and Tox4-associated proteins by mass spectrometry. Inducible T-REx HEK293 stable cell lines that express FLAG-PNUTS, FLAG-Tox4, or empty vector were induced with 1 μg/ml doxycycline for 3 days. Nuclear extracts were prepared and subjected to FLAG immunoprecipitation, and bound proteins were eluted by FLAG peptide after extensive washing. Proteins were analyzed by SDS-PAGE and stained with Coomassie Brilliant Blue. Specific bands were analyzed by mass spectrometry. The *arrows* indicate identified proteins. *B*, summary of the PTW/PP1 phosphatase complex. The domain structure of each component in the PTW/PP1 phosphatase complex is schematically shown. *TFS2N*, transcription factor II N-terminal domain; *RVXF motif*, PP1 docking motif; *Zinc finger*; *HMG box*, high mobility group box; *PP2Ac*, catalytic domain of protein phosphatase 2A; *WD40*, WD40 repeat. The number of amino acids in each component is indicated.

with Tox4, Wdr82, the PP1 catalytic subunits, and Hsp70. Tox4 associates with PNUTS, Wdr82, the PP1 catalytic subunits, Hsp70, and Vimentin. These data reveal that PNUTS and Tox4 are primarily associated with the PTW/PP1 complex *in vivo*. Taken together, data from co-immunoprecipitation, sucrose gradient fractionation analysis, and identification of Wdr82-, PNUTS-, and Tox4-associated proteins by mass spectrometry indicate that PNUTS, Tox4, Wdr82, and PP1 comprise a stable PTW/PP1 complex.

Protein Domains within the PTW/PP1 Phosphatase Complex—Data base searches indentified candidate orthologues of Wdr82 and PP1 in yeast and metazoa. However, candidate orthologues for PNUTS and Tox4 are found in *Xenopus* and *Drosophila* but not in yeast (data not shown). This indicates that the PTW phosphatase complex is specific for metazoa. Primary sequence analysis reveals that PNUTS possesses a TFS2N domain in its N terminus, a central RV*X*F motif, and a single putative zinc finger with the signature C-X_8-C-X_5-C-X_3-H at its extreme C terminus (Fig. 3*B*). The TFS2N domain is found in transcription elongation factor S-II, elongin A, and mediator complex subunit 26 and is implicated in the transcriptional initiation or elongation of RNA pol II (19). Tox4, a member of the TOX high mobility group box subfamily, possesses an high mobility group box implicated in protein-protein interactions and binding to bent or distorted DNA, such as four-way DNA junctions (53). The PP1 catalytic subunit harbors the catalytic domain specific to phosphorylated serine or threonine (1–3). Wdr82 contains seven WD40 domains, which are implicated in recognition of post-translational modifications of proteins such as phosphorylated serine or threonine and methylated lysine (28, 29, 30, 31, 34). This domain structure suggests that the PTW/PP1 phosphatase complex may be involved in regulating chromatin structure in the nucleus.

Molecular Interactions within the PTW/PP1 Phosphatase Complex—To gain insights into the molecular interactions within the PTW/PP1 phosphatase complex, epitope-tagged versions of each component were purified and used for *in vitro* pull-down analysis. Fig. 4*A* reveals that FLAG-Wdr82 directly interacts with PNUTS but does not directly interact with PP1α and Tox4. Importantly, Wdr82 successfully pulls down PP1α in the presence of PNUTS, indicating that PNUTS mediates the association between Wdr82 and PP1α. In addition, GST-PP1α directly interacts with PNUTS but does not interact with Wdr82 and Tox4 (Fig. 4*B*). Importantly, PP1α interacts with Wdr82 in the presence of PNUTS, indicating that PNUTS mediates the association between PP1α and Wdr82. Thus, these results indicate that PNUTS directly interacts with Wdr82 and PP1 but that there are no direct interactions between Tox4, Wdr82, and PP1.

Truncated fragments of PNUTS were similarly analyzed to further investigate interactions between PNUTS and Tox4, Wdr82, and PP1. Various deletion constructs of PNUTS carrying an N-terminal FLAG epitope were transiently transfected into HEK293 cells. Nuclear extracts were prepared and subjected to FLAG immunoprecipitation, and immunoprecipitates were analyzed by Western blotting. Fig. 4*C* confirms that full-length FLAG-PNUTS interacts with endogenous Tox4, Wdr82, and PP1. Wdr82 is immunoprecipitated by N-terminal (aa 1–619) and C-terminal (aa 418–888) fragments of PNUTS but not by PNUTS fragments containing aa 1–465 or 465–888. Thus, these results reveal that the middle region of PNUTS (aa 418–619) is required for the interaction with Wdr82. PP1 is immunoprecipitated by PNUTS fragments containing aa 1–465 and 388–888 but not by PNUTS fragments containing aa 1–348 or 418–888. Thus, these results indicate that the aa 388–417 region of PNUTS is required for interaction with PP1. This region contains the previously described RVXF PP1-interaction motif of PNUTS (20, 21) (Fig. 4*D*). Last, Tox4 interacts with all C-terminal deletion PNUTS fragments but does not interact following deletion of aa 1–114, indicating that Tox4 interacts with the N-terminal region of PNUTS. This result is consistent with a previous yeast two-hybrid result that showed that the N-terminal region of PNUTS interacts with Tox4 (54). Consistent with the failure to detect direct interactions between Tox4, Wdr82, and PP1 *in vitro* (Fig. 3, *A* and *B*), the N-terminal fragment of PNUTS (aa 1–348) interacts with Tox4 but does not immunoprecipitate either PP1α or Wdr82. Similarly, the C-terminal fragment of PNUTS (aa 418–888) interacts with Wdr82 but does not immunoprecipitate either Tox4 or PP1α. Taken together, these results indicate that PNUTS mediates PTW/PP1 complex formation by providing distinct binding platforms to each component.

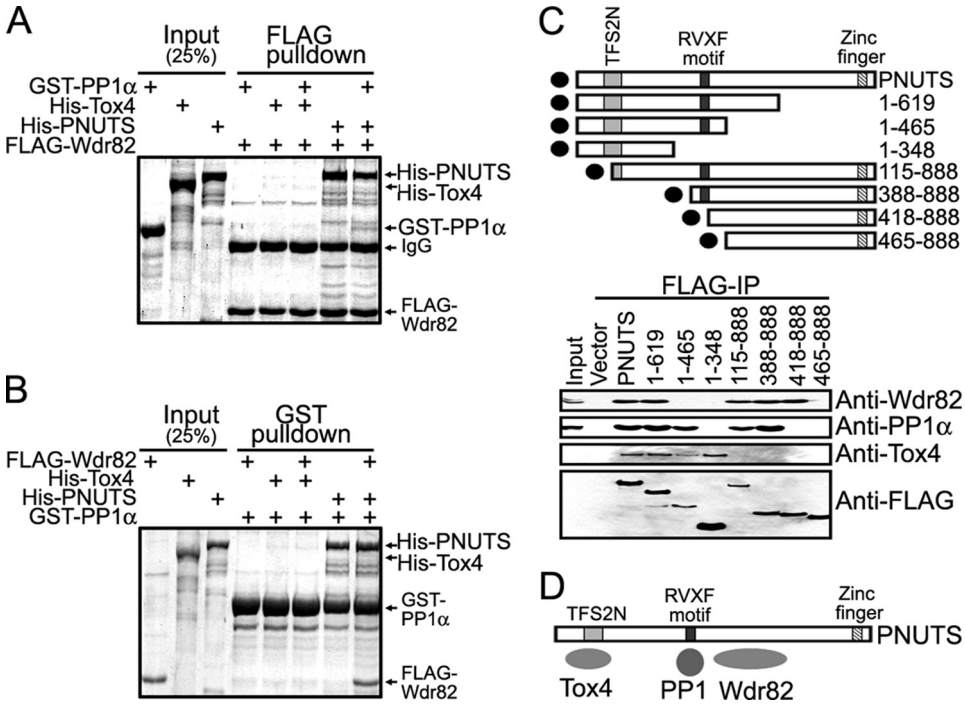

FIGURE 4. **PNUTS mediates PTW/PP1 complex formation by providing a binding platform to each component.** *A*, PNUTS directly interacts with Wdr82 and mediates the association of Wdr82 with PP1α. Recombinant FLAG-Wdr82, His-PNUTS, and His-Tox4 were purified from insect *Sf9* cells, and GST-PP1α was purified from *E. coli*. Purified FLAG-Wdr82 was incubated with various combinations of purified components, and protein interactions were analyzed by *in vitro* FLAG pull-down assay. Proteins were separated by SDS-PAGE and detected by Coomassie Brilliant Blue staining. The *arrows* indicate identities of protein bands. *B*, PNUTS directly interacts with PP1α and mediates the association of PP1α with Wdr82. Purified GST-PP1α was incubated with various combinations of purified components, and protein interactions were analyzed by an *in vitro* GST pull-down assay. Proteins were analyzed as described above. *C*, protein-protein interactions within the PTW/PP1 phosphatase complex. A diagram of PNUTS deletion constructs is shown. The *numbers* indicate amino acid residues of the PNUTS protein. HEK293 cells were transiently transfected with various deletion constructs of PNUTS with an N-terminal FLAG epitope. Nuclear extracts were prepared and subjected to FLAG immunoprecipitation (*FLAG-IP*), and immunoprecipitates were analyzed by Western blotting using the indicated antisera. *D*, summary of protein-protein interactions within the PTW/PP1 phosphatase complex.

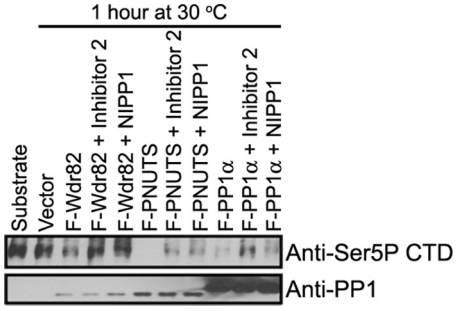

FIGURE 5. **The PTW/PP1 complex exhibits phosphatase activity *in vitro*.** Wdr82-, PNUTS-, and PP1α-associated proteins were purified from inducible T-REx HEK293 cell lines using FLAG immunoprecipitation. Purified proteins were examined in a phosphatase assay, using GST-CTD phosphorylated by MAPK as a substrate. *In vitro* phosphorylated GST-CTD was incubated with the immunoprecipitate from vector control, Wdr82, PNUTS, or PP1α in the absence or presence of the PP1-specific inhibitor NIPP1 or inhibitor 2 at 30 °C for 1 h. Reaction products were analyzed by Western blotting using anti-Ser(P)^5 (*Anti-Ser5P*) CTD and anti-PP1α antisera. The anti-Ser(P)^5 CTD antiserum recognizes phosphorylated CTD at Ser^5, the major product of the MAPK reaction (34). The slightly slower mobility of PP1 in the PP1 immunoprecipitates is due to the presence of the FLAG epitope.

The PTW/PP1 Complex Exhibits Phosphatase Activity in Vitro—PP1 has been reported to dephosphorylate the CTD of RNA pol II large subunit *in vitro* (55). Studies were performed to assess the phosphatase activity of the PTW/PP1 complex using phosphorylated GST-CTD as a substrate. Wdr82-, PNUTS-, and PP1α-associated proteins were purified by FLAG immunoprecipitation from HEK293 cells, as described above, and analyzed for phosphatase activity. Phosphorylated GST-CTD was incubated with Wdr82, PNUTS, or PP1α immunoprecipitates in the absence or presence of the PP1-specific inhibitors NIPP1 (45) or inhibitor 2 (44) (Fig. 5). The level of phosphorylated GST-CTD was analyzed by Western blotting using phosphorylation-specific antiserum. The Wdr82, PNUTS, and PP1α immunoprecipitates each dephosphorylated the GST-CTD substrate, and this phosphatase activity was partially blocked by the presence of PP1 inhibitors. Also, the amount of the PP1 catalytic subunit in the PNUTS immunoprecipitate is far less than the PP1α immunoprecipitate, but these samples exhibit comparable phosphatase activity, demonstrating that the PTW/PP1 complex efficiently dephosphorylates GST-CTD *in vitro*. These results confirm that the PTW/PP1 complex exhibits PP1-dependent protein phosphatase activity.

Chromatin Association and Integrity of the PTW/PP1 Phosphatase Complex throughout Cell Cycle Progression—Protein domains within the PTW/PP1 phosphatase complex (*e.g.* the TFS2N domain of PNUTS and the high mobility group box domain of Tox4) suggest that the complex functions in chromatin regulation. Additional experiments were performed to determine whether the PTW/PP1 phosphatase complex is associated with chromatin throughout cell cycle progression. T-REx HEK293 cells that express FLAG-PNUTS were stained with anti-FLAG antibody and observed using confocal microscopy. Consistent with a previous report (21), FLAG-PNUTS associates with chromatin during interphase, is excluded from condensed chromosomes during early mitosis, and is reloaded onto chromosomes at late telophase (Fig. 6*A*). To further assess the chromatin association of the complex, we performed *in vitro* sequential biochemical fractionation experiments as described previously (21, 42). HEK293 cells were successively extracted to recover soluble, chromatin-associated, and matrix-associated protein fractions, and an equal proportion of each fraction was analyzed by Western blotting. Consistent with a previous report (21), endogenous PNUTS and Tox4 are nearly exclusively associated with the chromatin-associated protein fraction (Fig. 6*B*). Wdr82 is predominantly associated with chromatin- and matrix-associated protein fractions, indicating that Wdr82-containing complexes are associated with chro-

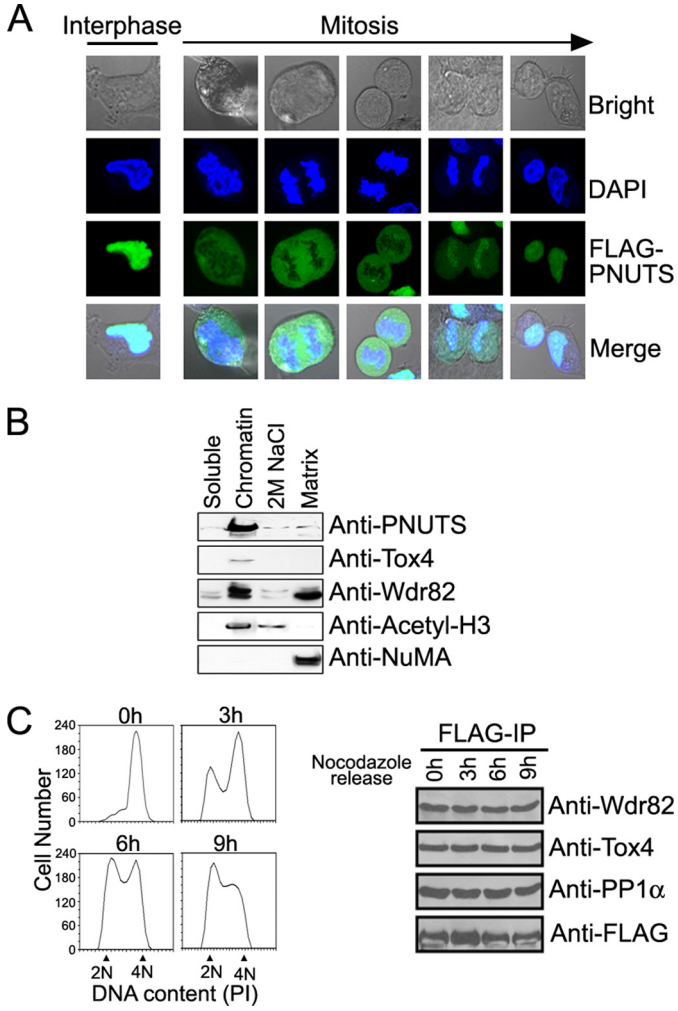

FIGURE 6. **Chromatin association and integrity of the PTW/PP1 complex throughout cell cycle progression.** *A*, chromatin association of PNUTS is regulated throughout cell cycle progression. Inducible T-REx HEK293 cells that express FLAG-PNUTS were cultured on glass bottom collagen-coated dishes and induced by 1 μg/ml doxycycline for 2 days. Cells were stained with anti-FLAG antibody and fluorescein isothiocyanate (FITC)-conjugated secondary antibody. Cells were observed by confocal microscopy after DNA was stained with DAPI. Cell phase was determined based on cell morphology and DAPI stains. *B*, the PTW/PP1 phosphatase complex is associated with chromatin. HEK293 cells were fractionated by sequential extraction as described previously (42). An equal proportion of each fraction was analyzed by Western blotting. Acetylated histone H3 and NuMA were used as marker proteins for chromatin and matrix fractions, respectively. *C*, the integrity of the PTW/PP1 phosphatase complex is preserved throughout cell cycle progression. T-REx HEK293 cells expressing FLAG-PNUTS were induced and synchronized by successive thymidine-nocodazole block. Cells were harvested at various time points following release from arrest. A small fraction of cells at each time point was analyzed for cell cycle distribution by PI staining and flow cytometry. Whole cell extracts were prepared and subjected to FLAG immunoprecipitation (*FLAG-IP*), and immunoprecipitates were analyzed by Western blotting using the indicated antisera.

matin or matrix. NuMA and acetylated histone H3 were used as marker proteins of the matrix and chromatin-associated protein fractions, respectively (42). Therefore, data from analysis of localization and sequential biochemical fractionation indicate that chromatin association of the PTW/PP1 complex is regulated during cell cycle progression.

To examine the integrity of the PTW/PP1 phosphatase complex during cell cycle progression, T-REx HEK293 cells expressing FLAG-PNUTS were synchronized by successive thymidine-nocodazole block and harvested at various time points following release from cell cycle arrest. Cell cycle analysis indicates that at least 90% of cells were synchronized at the mitotic block (0 h) and progressively moved to G_1 and S phases (3, 6, and 9 h) (Fig. 6*C*). Whole cell extracts were prepared from cells at each time point and subjected to FLAG immunoprecipitation, and immunoprecipitates were analyzed by Western blotting. PNUTS was found to immunoprecipitate Tox4, Wdr82, and PP1 at the mitotic block (0 h) and at all times tested following nocodazole release (3, 6, and 9 h). Similar results were observed at 1, 12, and 24 h after nocodazole release (data not shown). These data indicate that although chromatin association of the PTW/PP1 complex is dynamically regulated throughout the cell cycle, the integrity of the PTW/PP1 phosphatase complex is intact throughout cell cycle progression.

Dysregulation of the PTW/PP1 Phosphatase Complex Causes Cell Cycle Arrest—To investigate the physiologic functions of the PTW/PP1 phosphatase complex, we tested whether a PP1 interaction-defective form of PNUTS (W401A) (20, 21) can be used as a dominant negative mutant. Inducible T-REx HEK293 cells that express FLAG-PNUTS (W401A) were developed. FLAG immunoprecipitates were analyzed by Western blotting to assess the ability of the PNUTS (W401A) protein to interact with other components of the PTW/PP1 complex (Fig. 7*A*). Consistent with a previous report (20), the PNUTS (W401A) mutant fails to interact with PP1 but still interacts with Tox4 and Wdr82. These results are consistent with our previous observation that Tox4, Wdr82, and PP1 interact with distinct PNUTS domains (Fig. 4).

T-REx HEK293 cells that express empty vector or FLAG-PNUTS did not show any proliferation defects upon transgene induction. However, although inducible cell lines expressing mutant FLAG-PNUTS (W401A) appear normal prior to transgene induction, they exhibit a proliferation defect following induction (Fig. 7*B*). Cells start to detach from tissue culture dishes within 2 days of induction, and after 4.5 days of induction, a majority of cells show morphological features of cell death, including condensed chromatin, nuclear fragmentation, cell shrinkage, and cell blebbing, indicating that expression of the PNUTS (W401A) mutant leads to cell death (Fig. 7*C*). To further characterize the mechanism of cell death, cells were analyzed by flow cytometry after staining with Annexin V and PI. Consistent with Fig. 7*C*, cells expressing the PNUTS (W401A) mutant for 3 days showed an elevated level (23.1%) of dead cells compared with control cells (5.9%) (Fig. 7*D*). Also, ~9.1% of cells expressing the PNUTS (W401A) mutant were undergoing apoptosis (Annexin V-positive, PI-negative), in contrast to ~4.3% of control cells. These data indicate that expression of the PNUTS (W401A) mutant causes apoptotic cell death.

Cell cycle distribution was analyzed to further characterize the proliferation defects caused by the PNUTS (W401A) mutant (Fig. 7*E*). Cells do not show cell cycle defects prior to induction of FLAG-PNUTS (W401A) but exhibit a dramatic increase of cells in G_2/M phase and decrease of cells in S phase 3 days following induction. This indicates that expression of the PP1 interaction-defective form of PNUTS (W401A) causes cell

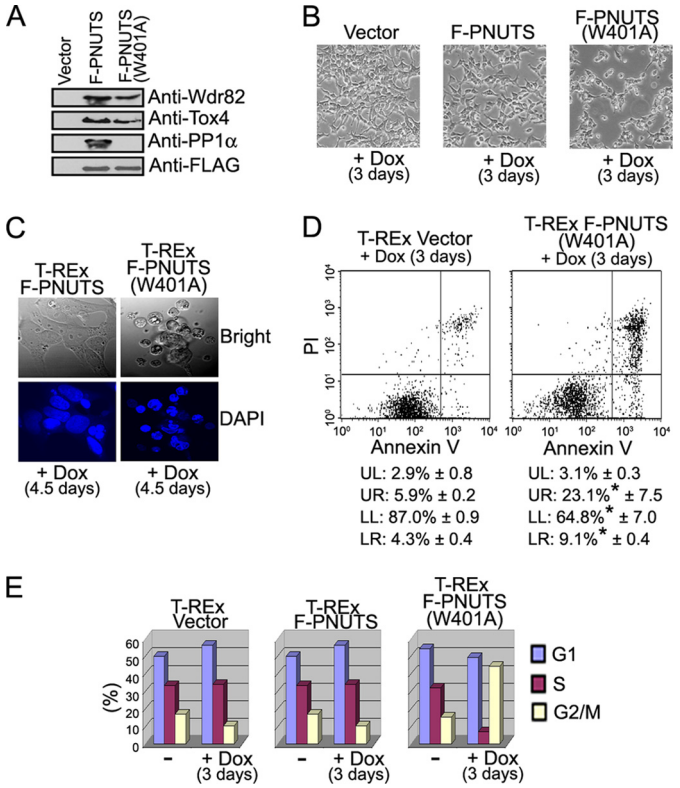

FIGURE 7. **Dysregulation of the PTW/PP1 phosphatase complex causes cell cycle arrest and cell death.** *A*, the PNUTS (W401A) mutant interacts with Wdr82 and Tox4 but not with PP1. T-REx HEK293 cell lines that express FLAG-PNUTS, FLAG-PNUTS (W401A), or empty vector were induced with 1 μg/ml doxycycline for 3 days. Nuclear extracts were subjected to FLAG immunoprecipitation, and immunoprecipitates were analyzed by Western blotting. *B*, inducible expression of PNUTS (W401A) causes proliferation defects. T-REx HEK293 cell lines that express empty vector, FLAG-PNUTS, or FLAG-PNUTS (W401A) were cultured in the presence of 1 μg/ml doxycycline for 3 days. Cell morphology was photographed using inverted microscopy. Representative images are shown. *C*, inducible expression of PNUTS (W401A) leads to cell death. T-REx HEK293 cell lines that express FLAG-PNUTS or FLAG-PNUTS (W401A) were cultured on glass bottom collagen-coated dishes. Cells were induced with 1 μg/ml doxycycline for 4.5 days. Cells were fixed and stained by DAPI and observed by confocal microscopy. Representative images are shown. *D*, inducible expression of PNUTS (W401A) leads to apoptotic cell death. T-REx HEK293 cell lines that express empty vector or FLAG-PNUTS (W401A) were cultured in the presence of 1 μg/ml doxycycline for 3 days. Apoptotic cells were detected by flow cytometry after Annexin V and PI staining. *UR*, *upper right panel* corresponding to dead cells; *LL*, *lower left panel* corresponding to healthy cells; *LR*, *lower right panel* corresponding to apoptotic cells. *Numerical values* represent a summary of data from three experiments. *, $p < 0.05$. *E*, inducible expression of PNUTS (W401A) causes cell cycle arrest. T-REx HEK293 cell lines that express empty vector, FLAG-PNUTS, or FLAG-PNUTS (W401A) were cultured in the absence or the presence of 1 μg/ml doxycycline for 3 days. Cells were analyzed for cell cycle distribution by PI staining and flow cytometry. The percentage of cells in each phase of the cell cycle was determined.

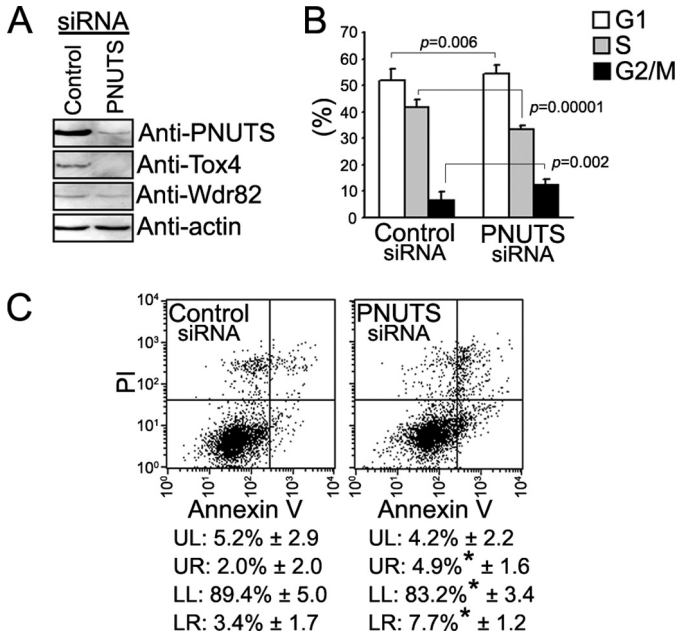

FIGURE 8. **Depletion of PNUTS results in destabilization of the PTW/PP1 complex leading to cell cycle dysregulation and apoptotic cell death.** *A*, depletion of PNUTS causes destabilization of the PTW/PP1 complex. HEK293 cells were transfected with control or PNUTS siRNA pools according to the manufacturer's instructions. Proteins were analyzed by Western blotting after 3 days of transfection. *B*, depletion of PNUTS causes abnormal cell cycle distribution. Cell cycle distribution after 3 days of transfection was analyzed by PI staining and flow cytometry. The *error bars* indicate the mean S.D., and *p* values were determined by a standard *t* test. *C*, depletion of PNUTS causes apoptotic cell death. Apoptotic cells after 3 days of transfection were analyzed by cytometry after Annexin V and PI staining. *UR*, *upper right panel* corresponding to dead cells; *LL*, *lower left panel* corresponding to healthy cells; *LR*, *lower right panel* corresponding to apoptotic cells. *Numerical values* represent a summary of data from three experiments. *, $p < 0.05$.

cycle arrest at G_2/M phase and blocks cell cycle progression into S phase.

To further investigate the function of the PTW/PP1 complex, we depleted PNUTS, the scaffold protein of the complex, by siRNA in HEK293 cells. Whole cell extracts were prepared 3 days following transfection and analyzed by Western blotting. An ~90% decrease of PNUTS protein was observed following transfection with PNUTS-specific siRNA compared with non-specific siRNA control (Fig. 8*A*). Depletion of PNUTS also led to a nearly complete loss of Tox4 and to reduced levels of the Wdr82 component of the PTW/PP1 complex but did not affect the expression level of actin. Consistent with Fig. 4, this result provides additional evidence of PNUTS function as a scaffolding protein in the PTW/PP1 complex. These results indicate that depletion of PNUTS causes destabilization of the PTW/PP1 complex.

Cell cycle distribution was analyzed for PNUTS-depleted cells after 3 days of transfection (Fig. 8*B*). Similar to cells expressing the PP1 interaction-defective PNUTS (W401A) mutant, PNUTS-depleted cells exhibited an abnormal cell cycle distribution, with significant increases of cells in G_2/M and G_1 phases and a significant decrease of cells in S phase. This indicates that dysregulation of the PTW/PP1 complex causes cell cycle arrest at G_2/M phase and blocks cell cycle progression into S phase. PNUTS-depleted cells were also analyzed by flow cytometry after staining with Annexin V and PI (Fig. 8*C*). Similar to cells expressing the PNUTS (W401A) mutant, PNUTS-depleted cells showed significant increases of dead and apoptotic cells compared with control cells. This result indicates that dysregulation of the PTW/PP1 complex causes apoptotic cell death.

T-REx HEK293 cells that express GFP-PNUTS (W401A) were developed to further examine the observed cell cycle defect and apoptotic cell death. Cells expressing GFP-PNUTS (W401A) for 3 days showed proliferation defects similar to those shown for cells that express FLAG-PNUTS (W401A) (data not shown). Cells were fixed and stained by DAPI and

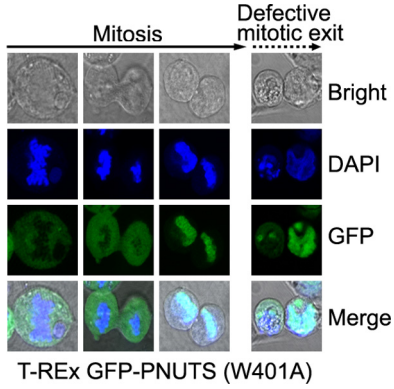

FIGURE 9. **Dysregulation of the PTW/PP1 phosphatase complex causes defects at mitotic exit.** T-REx HEK293 cells that express GFP-PNUTS (W401A) were cultured on glass bottom collagen-coated dishes. Cells were cultured in the presence of 1 μg/ml doxycycline for 3 days. Cells were fixed and stained by DAPI and observed by confocal microscopy. The *first three columns* show representative progression through mitotic stages, and the *fourth column* shows a representative image of a defective exit from mitosis to interphase.

observed using confocal microscopy. Similar to wild type PNUTS, the GFP-PNUTS (W401A) mutant associates with chromatin in interphase, is excluded from condensed chromosomes during early mitosis, and is reloaded into chromosomes at late telophase (Fig. 9). However, after its loading into chromosomes at the exit of mitosis, the GFP-PNUTS (W401A) mutant causes partial and uneven chromatin decondensation, leading to cell cycle arrest at mitotic exit and subsequent apoptotic cell death. These results indicate that the PTW/PP1 phosphatase complex is essential for the transition from mitosis to interphase and suggest that this complex plays a role in chromatin remodeling.

DISCUSSION

Wdr82, a WD40 domain-containing protein, was previously identified as an integral component of the human Setd1a and Setd1b histone H3-Lys^4 methyltransferase complexes and mediates the interaction of these complexes with initiating and early elongating RNA pol II by recognizing Ser^5-phosphorylated CTD (32–34). The data reported here reveal that Wdr82 additionally associates with other protein complexes, including the Mll3 and Mll4 histone H3-Lys^4 methyltransferases, the PTW/PP1 phosphatase complex, and the chaperonin-containing Tcp1 complex. Previously, several groups identified the Mll3 and Mll4 complexes, but Wdr82 was not found (48, 49, 56). Mll3 and Mll4 proteins lack the RRM domain through which Wdr82 interacts with the Setd1a and Setd1b proteins. Thus, the mechanism of interaction between Wdr82 and Mll3/4 and whether Wdr82 similarly targets these methyltransferases to Ser^5-phosphorylated CTD remain to be determined. The Tcp1 complex is required for structural formation of WD40 domain-containing proteins (57); thus, it is not surprising to find this interaction with Wdr82.

The PTW/PP1 phosphatase complex is a newly identified multimeric PP1 complex. Interestingly, Swd2, a homologue of mammalian Wdr82, is a component of the yeast Set1/COMPASS histone H3-Lys^4 methyltransferase complex as well as the APT complex (35–38). The APT complex consists of six protein components (Pti1, Swd2, Glc7, Ssu72, Ref2, and Syc1) and is implicated in the transcription termination of small nucleolar RNA genes in yeast (39). Importantly, Glc7, the yeast homologue of PP1, is present in a stable complex with Swd2. Thus, although the PNUTS and Tox4 components of the mammalian PTW/PP1 phosphatase complex do not show homology to components of the yeast APT complex, the presence of Wdr82 homologues in PP1 complexes is conserved from yeast to mammals. Wdr82 may function to recognize phosphorylated serine/threonine residues for PP1 action, consistent with our previous report that Wdr82 in the Setd1a and Setd1b methyltransferase complexes specifically recognizes Ser^5-phosphorylated RNA pol II CTD (34).

Analysis of the PTW/PP1 phosphatase complex shows that PNUTS serves as a binding platform for complex formation and is mainly present as a stable complex *in vivo*. This result is also supported by reports from other groups. Trinkle-Mulcahy *et al.* (50) stably expressed each of the PP1 catalytic isoforms in HeLa cells and purified PP1-associated proteins by immunopurification. They identified numerous PP1-interacting proteins by mass spectrometry, including PNUTS, Tox4, and Wdr82. Kreivi *et al.* (16) purified a high molecular weight PP1 complex from HeLa cell nuclear extracts using conventional and affinity chromatography. The purified fraction contained six major proteins, two of which corresponded to PNUTS and PP1. Although not further characterized, the protein profile obtained is similar to the profiles we observed following affinity purification of PNUTS- and Tox4-associated proteins (Fig. 3*A*). It was also shown by yeast two-hybrid screening that the N-terminal region of PNUTS interacts with Tox4 (54). PNUTS is ubiquitously expressed and is implicated in multiple cellular pathways, including chromosome decondensation, cell cycle progression, and apoptosis (21–25). The finding that PNUTS associates predominantly with PTW/PP1 complex components suggests that these PNUTS functions may be mediated via the PTW/PP1 phosphatase complex.

Functional inactivation of PP1 results in mitotic arrest or deficient cytokinesis in mammalian cells (3, 8, 9). Although a large number of mitotic phosphoproteins are known to be dephosphorylated by PP1, the relevant PP1 holoenzyme complexes or regulatory subunits have not been identified. It was shown that PNUTS is imported into the nucleus after cells form intact nuclear membranes and that PNUTS associates with chromosomes at mitotic exit. Also, dephosphorylation of phosphoserine 10 of histone H3 precedes chromosome association of PNUTS during mitotic exit (21). Using inducible cell lines, we demonstrate that a PP1 interaction-defective form of PNUTS (W401A) associates with chromosomes but causes abnormal chromatin structures at mitotic exit, eventually leading to apoptotic cell death. Expression of the PNUTS (W401A) mutant does not affect PP1-mediated mitotic processes, such as chromosome condensation, chromosome segregation, and cytokinesis. This observation suggests that the PTW/PP1 phosphatase complex is critical for mitotic exit, possibly by regulating chromosome decondensation as previously proposed by Landsverk *et al.* (21). The identity of *in vivo* substrates of the PTW/PP1 phosphatase complex and how this complex is regulated during the transition between mitosis and interphase remain to be determined. We showed that the integrity of the

complex is intact during cell cycle progression. Interestingly, PP1 catalytic subunits are subject to reversible phosphorylation at threonine 320, resulting in regulation of enzyme activity during the burst of protein dephosphorylation that occurs at the transition between interphase and mitosis (58, 59). PNUTS is also reported to be phosphorylated (20). Taken together, these findings suggest that phosphatase activity of the PTW/PP1 complex may be regulated by phosphorylation and dephosphorylation cascades to ensure cell cycle progression and mitotic exit.

Acknowledgments—We thank Mathieu Bollen (Catholic University of Leuven, Belgium) for generously providing a rabbit polyclonal PNUTS antibody. Antisera directed against Mll4 and Ptip were a kind gift of Kai Ge (NIDDK, National Institutes of Health). We thank Dr. Michael Dahmus (University of California, Davis, CA) for providing pGST-mCTD and Dr. Anna DePaoli-Roach (Indiana University) for helpful discussions.

REFERENCES

1. Shenolikar, S. (1994) *Annu. Rev. Cell Biol.* **10,** 55–86
2. Aggen, J. B., Nairn, A. C., and Chamberlin, R. (2000) *Chem. Biol.* **7,** R13–R23
3. Ceulemans, H., and Bollen, M. (2004) *Physiol. Rev.* **84,** 1–39
4. Andreassen, P. R., Lacroix, F. B., Villa-Moruzzi, E., and Margolis, R. L. (1998) *J. Cell Biol.* **141,** 1207–1215
5. Trinkle-Mulcahy, L., Sleeman, J. E., and Lamond, A. I. (2001) *J. Cell Sci.* **114,** 4219–4228
6. Cohen, P. T. (2002) *J. Cell Sci.* **115,** 241–256
7. Virshup, D. M., and Shenolikar, S. (2009) *Mol. Cell* **33,** 537–545
8. Fernandez, A., Brautigan, D. L., and Lamb, N. J. (1992) *J. Cell Biol.* **116,** 1421–1430
9. Cheng, A., Dean, N. M., and Honkanen, R. E. (2000) *J. Biol. Chem.* **275,** 1846–1854
10. Trinkle-Mulcahy, L., Andrews, P. D., Wickramasinghe, S., Sleeman, J., Prescott, A., Lam, Y. W., Lyon, C., Swedlow, J. R., and Lamond, A. I. (2003) *Mol. Biol. Cell* **14,** 107–117
11. Skoufias, D. A., Indorato, R. L., Lacroix, F., Panopoulos, A., and Margolis, R. L. (2007) *J. Cell Biol.* **179,** 671–685
12. Bollen, M., Gerlich, D. W., and Lesage, B. (2009) *Trends Cell Biol.* **19,** 531–541
13. De Wulf, P., Montani, F., and Visintin, R. (2009) *Curr. Opin. Cell Biol.* **21,** 806–815
14. Wu, J. Q., Guo, J. Y., Tang, W., Yang, C. S., Freel, C. D., Chen, C., Nairn, A. C., and Kornbluth, S. (2009) *Nat. Cell Biol.* **11,** 644–651
15. Bennett, D. (2005) *Biochem. Soc. Trans.* **33,** 1444–14446
16. Kreivi, J. P., Trinkle-Mulcahy, L., Lyon, C. E., Morrice, N. A., Cohen, P., and Lamond, A. I. (1997) *FEBS Lett.* **420,** 57–62
17. Allen, P. B., Kwon, Y. G., Nairn, A. C., and Greengard, P. (1998) *J. Biol. Chem.* **273,** 4089–4095
18. Raha-Chowdhury, R., Andrews, S. R., and Gruen, J. R. (2005) *Brain Res. Mol. Brain Res.* **138,** 70–83
19. Booth, V., Koth, C. M., Edwards, A. M., and Arrowsmith, C. H. (2000) *J. Biol. Chem.* **275,** 31266–31268
20. Kim, Y. M., Watanabe, T., Allen, P. B., Kim, Y. M., Lee, S. J., Greengard, P., Nairn, A. C., and Kwon, Y. G. (2003) *J. Biol. Chem.* **278,** 13819–13828
21. Landsverk, H. B., Kirkhus, M., Bollen, M., Küntziger, T., and Collas, P. (2005) *Biochem. J.* **390,** 709–717
22. Udho, E., Tedesco, V. C., Zygmunt, A., and Krucher, N. A. (2002) *Biochem. Biophys. Res. Commun.* **297,** 463–467
23. Krucher, N. A., Rubin, E., Tedesco, V. C., Roberts, M. H., Sherry, T. C., and De Leon, G. (2006) *Exp. Cell Res.* **312,** 2757–2763
24. De Leon, G., Sherry, T. C., and Krucher, N. A. (2008) *Cancer Biol. Ther.* **7,** 833–841
25. Lee, S. J., Lim, C. J., Min, J. K., Lee, J. K., Kim, Y. M., Lee, J. Y., Won, M. H., and Kwon, Y. G. (2007) *Cell Death Differ.* **14,** 1106–1116
26. Smith, T. F., Gaitatzes, C., Saxena, K., and Neer, E. J. (1999) *Trends Biochem. Sci.* **24,** 181–185
27. Li, D., and Roberts, R. (2001) *Cell. Mol. Life Sci.* **58,** 2085–2097
28. Couture, J. F., Collazo, E., and Trievel, R. C. (2006) *Nat. Struct. Mol. Biol.* **13,** 698–703
29. Ruthenburg, A. J., Wang, W., Graybosch, D. M., Li, H., Allis, C. D., Patel, D. J., and Verdine, G. L. (2006) *Nat. Struct. Mol. Biol.* **13,** 704–712
30. Orlicky, S., Tang, X., Willems, A., Tyers, M., and Sicheri, F. (2003) *Cell* **112,** 243–256
31. Wu, G., Xu, G., Schulman, B. A., Jeffrey, P. D., Harper, J. W., and Pavletich, N. P. (2003) *Mol. Cell* **11,** 1445–1456
32. Lee, J. H., and Skalnik, D. G. (2005) *J. Biol. Chem.* **280,** 41725–41731
33. Lee, J. H., Tate, C. M., You, J. S., and Skalnik, D. G. (2007) *J. Biol. Chem.* **282,** 13419–13428
34. Lee, J. H., and Skalnik, D. G. (2008) *Mol. Cell. Biol.* **28,** 609–618
35. Nedea, E., He, X., Kim, M., Pootoolal, J., Zhong, G., Canadien, V., Hughes, T., Buratowski, S., Moore, C. L., and Greenblatt, J. (2003) *J. Biol. Chem.* **278,** 33000–33010
36. Cheng, H., He, X., and Moore, C. (2004) *Mol. Cell. Biol.* **24,** 2932–2943
37. Dichtl, B., Aasland, R., and Keller, W. (2004) *RNA* **10,** 965–977
38. Roguev, A., Shevchenko, A., Schaft, D., Thomas, H., Stewart, A. F., and Shevchenko, A. (2004) *Mol. Cell. Proteomics* **3,** 125–132
39. Nedea, E., Nalbant, D., Xia, D., Theoharis, N. T., Suter, B., Richardson, C. J., Tatchell, K., Kislinger, T., Greenblatt, J. F., and Nagy, P. L. (2008) *Mol. Cell* **29,** 577–587
40. Lee, J. S., Shukla, A., Schneider, J., Swanson, S. K., Washburn, M. P., Florens, L., Bhaumik, S. R., and Shilatifard, A. (2007) *Cell* **131,** 1084–1096
41. Vitaliano-Prunier, A., Menant, A., Hobeika, M., Géli, V., Gwizdek, C., and Dargemont, C. (2008) *Nat. Cell Biol.* **10,** 1365–1371
42. Lee, J. H., and Skalnik, D. G. (2002) *J. Biol. Chem.* **277,** 42259–42267
43. Simon, V. R., and Moran, M. F. (2001) *Cell Prolif.* **34,** 15–30
44. Hurley, T. D., Yang, J., Zhang, L., Goodwin, K. D., Zou, Q., Cortese, M., Dunker, A. K., and DePaoli-Roach, A. A. (2007) *J. Biol. Chem.* **282,** 28874–28883
45. Beullens, M., Van Eynde, A., Vulsteke, V., Connor, J., Shenolikar, S., Stalmans, W., and Bollen, M. (1999) *J. Biol. Chem.* **274,** 14053–14061
46. Wu, M., Wang, P. F., Lee, J. S., Martin-Brown, S., Florens, L., Washburn, M., and Shilatifard, A. (2008) *Mol. Cell. Biol.* **28,** 7337–7344
47. Dunn, A. Y., Melville, M. W., and Frydman, J. (2001) *J. Struct. Biol.* **135,** 176–184
48. Cho, Y. W., Hong, T., Hong, S., Guo, H., Yu, H., Kim, D., Guszczynski, T., Dressler, G. R., Copeland, T. D., Kalkum, M., and Ge, K. (2007) *J. Biol. Chem.* **282,** 20395–20406
49. Issaeva, I., Zonis, Y., Rozovskaia, T., Orlovsky, K., Croce, C. M., Nakamura, T., Mazo, A., Eisenbach, L., and Canaani, E. (2007) *Mol. Cell. Biol.* **27,** 1889–1903
50. Trinkle-Mulcahy, L., Andersen, J., Lam, Y. W., Moorhead, G., Mann, M., and Lamond, A. I. (2006) *J. Cell Biol.* **172,** 679–692
51. Shilatifard, A. (2008) *Curr. Opin. Cell Biol.* **20,** 341–348
52. Yeo, M., Lin, P. S., Dahmus, M. E., and Gill, G. N. (2003) *J. Biol. Chem.* **278,** 26078–26085
53. O'Flaherty, E., and Kaye, J. (2003) *BMC Genomics* **4,** 13–23
54. Lee, S. J., Lee, J. K., Maeng, Y. S., Kim, Y. M., and Kwon, Y. G. (2009) *Exp. Mol. Med.* **41,** 189–200
55. Washington, K., Ammosova, T., Beullens, M., Jerebtsova, M., Kumar, A., Bollen, M., and Nekhai, S. (2002) *J. Biol. Chem.* **277,** 40442–40448
56. Lee, M. G., Villa, R., Trojer, P., Norman, J., Yan, K. P., Reinberg, D., Di Croce, L., and Shiekhattar, R. (2007) *Science* **318,** 447–450
57. Yi, C., Li, S., Wang, J., Wei, N., and Deng, X. W. (2006) *Int. J. Biochem. Cell Biol.* **38,** 1076–1083
58. Dohadwala, M., da Cruz e Silva, E. F., Hall, F. L., Williams, R. T., Carbonaro-Hall, D. A., Nairn, A. C., Greengard, P., and Berndt, N. (1994) *Proc. Natl. Acad. Sci. U.S.A.* **91,** 6408–6412
59. Kwon, Y. G., Lee, S. Y., Choi, Y., Greengard, P., and Nairn, A. C. (1997) *Proc. Natl. Acad. Sci. U.S.A.* **94,** 2168–2173